

Supporting information for the article:

## **Label-Free, Visual Detection of Small Molecules Using Highly Target-Responsive Multi-Module Split Aptamer Constructs**

Yingping Luo,<sup>1,2</sup> Haixiang Yu,<sup>1</sup> Obtin Alkhamis,<sup>1</sup> Yingzhu Liu,<sup>1</sup> Xinhui Lou,<sup>3</sup> Boyang Yu<sup>2\*</sup>  
and Yi Xiao<sup>1\*</sup>

<sup>1</sup>Department of Chemistry and Biochemistry, Florida International University, 11200 SW 8th Street, Miami, FL, USA, 33199; <sup>2</sup>State Key Laboratory of Natural Medicines, Jiangsu Key Laboratory of TCM Evaluation and Translational Research, Department of Complex Prescription of TCM, China Pharmaceutical University, Nanjing 211198, P. R. China; <sup>3</sup>Department of Chemistry, Capital Normal University, Xisanhuan North Rd. 105, Beijing, China, 100048.

\*Corresponding authors: [yxiao2@fiu.edu](mailto:yxiao2@fiu.edu) and [boyangyucpu@163.com](mailto:boyangyucpu@163.com)

### **ABSTRACT**

Colorimetric aptamer-based sensors offer a simple means of on-site or point-of-care analyte detection. However, these sensors are largely incapable of achieving naked-eye detection due to the poor performance of the target-recognition and signal-reporting elements employed. To address this problem, we report a generalizable strategy for engineering novel multi-module split DNA constructs termed ‘CBSAzymes’ that utilize a cooperative binding split aptamer (CBSA) as a highly target-responsive bioreceptor and a new, highly-active split DNAzyme as an efficient signal reporter. CBSAzymes consist of two fragments that remain separate in the absence of target, but effectively assemble in the presence of target to form a complex that catalyzes the oxidation of 2,2'-azino-bis(3-ethylbenzthiazoline)-6-sulfonic acid, developing a dark green color within 5 minutes. Such assay enables rapid, sensitive, and visual detection of small-molecules, which has not been achieved with any previously-reported split-aptamer-DNAzyme conjugates. In an initial demonstration, we generate a cocaine-binding CBSAzyme that enables naked-eye detection of cocaine at concentrations as low as 10  $\mu$ M. Notably, CBSAzyme engineering is straightforward and generalizable. We demonstrate this by developing a methylenedioxypropylvalerone (MDPV)-binding CBSAzyme for visual detection of MDPV and 10 other synthetic cathinones at low micromolar concentrations, even in biological samples. Given that CBSAzyme-based assays are simple, label-free, rapid, robust, and instrument-free, we believe that such assays should be readily applicable for on-site visual detection of various important small molecules such as illicit drugs, medical biomarkers, and toxins in various sample matrices.

## Table of Contents

Experimental Section .....	S3
Materials .....	S3
Determination of split DNAzyme activity utilizing duplex DNA constructs .....	S3
Optimization of KCl and NaCl concentration.....	S3
Determination of CBSAzyme kinetics.....	S3
Characterizing binding affinity and cooperativity of MDPV-binding CBSA.....	S4
Circular dichroism characterization of CBSAzyme conformation .....	S4
Supporting Figures and Tables .....	S5
Figure S1 Optimization of the catalytic activity of duplex DNA-split DNAzyme conjugates.....	S5
Figure S2 Strategy for engineering the cocaine-binding CBSAzyme.....	S5
Figure S3 Effect of CBSA stem-length on the performance of the cocaine-detecting CBSAzyme .	S6
Figure S4 Determination of the enzyme kinetics of CBSAzyme with different split modes .....	S6
Figure S5 Circular dichroism spectra of CBSAzyme-5334-13.....	S7
Figure S6 Circular dichroism spectra of 1 $\mu$ M CBSAzyme-5334-22.....	S7
Figure S7 Optimization of the linker of CBSAzyme-5334-13 .....	S8
Figure S8 Circular dichroism spectra of COC-CBSAzyme.....	S8
Figure S9 Utilizing COC-CBSAzyme for the naked-eye detection of cocaine .....	S9
Figure S10 Optimization of the concentrations of both fragments of COC-CBSAzyme .....	S9
Figure S11 Comparison of the target-responsiveness of COC-CBSAzyme and SAzyme-334. ....	S10
Figure S12 Visual detection of cocaine using COC-CBSAzyme .....	S10
Figure S13 Specificity of the CBSAzyme-based assay for cocaine detection.....	S11
Figure S14 Design and performance of an MDPV-binding CBSAzyme.....	S11
Figure S15 Circular dichroism spectra of MDPV-CBSAzyme .....	S12
Figure S16-S18 Utilizing MDPV-CBSAzyme for the naked-eye detection of MDPV .....	S12-S13
Figure S19 Visual detection of MDPV in 50% saliva using MDPV-CBSAzyme.....	S14
Figure S20 Visual detection of MDPV in 50% urine using MDPV-CBSAzyme.....	S14
Figure S21 Target-cross-reactivity of the MDPV-CBSAzyme-based assay .....	S15
Figure S22 Specificity of the MDPV-CBSAzyme-based assay. ....	S15
Table S1 Oligonucleotide sequences used in this work.....	S16
Table S2 Comparison of this work to other aptamer-based assays for visual cocaine detection....	S17
References.....	S17

## EXPERIMENTAL SECTION

**Materials.** 2,2'-azino-bis(3-ethylbenzthiazoline)-6-sulfonic acid (ABTS), benzocaine, caffeine, chlorpromazine HCl, cocaine HCl, diphenhydramine HCl, levamisole HCl, lidocaine HCl, methamphetamine HCl, promazine HCl, scopolamine HCl, and sucrose were purchased from Sigma-Aldrich. Hemin was purchased from Frontier Scientific and prepared as a 5 mM stock solution in dimethyl sulfoxide (DMSO) and stored at  $-20\text{ }^{\circ}\text{C}$  before use. 30% hydrogen peroxide ( $\text{H}_2\text{O}_2$ ) was purchased from Fisher Scientific. Butylone, ethylone, 3,4-methylenedioxy- $\alpha$ -pyrrolidinobutiophenone, 3,4-methylenedioxypyrovalerone, mephedrone, methedrone, methylone, 4'-methyl- $\alpha$ -pyrrolidinobutiophenone, 4'-methyl- $\alpha$ -pyrrolidinohexanophenone, naphyrone, and pentylone were purchased from Cayman Chemical. All synthetic cathinones were purchased as hydrochloride salts. All other chemicals were purchased from Sigma-Aldrich unless otherwise specified. All DNA oligonucleotides were purchased from Integrated DNA Technologies. Oligonucleotides were dissolved in PCR grade water and DNA concentrations were measured with a NanoDrop 2000 (Thermo Scientific). The sequences are listed in the Electronic Supplementary Information (SI, Table S1).

**Determination of split DNAzyme activity utilizing duplex DNA constructs.** Duplex-DNA-DNAzyme conjugates were prepared by mixing strands A0 and B0, A1 and B0, A2 and B0, or A2 and B1 (0.25  $\mu\text{M}$  final concentration for each strand) in 40 mM HEPES buffer (pH 7.0) containing 50 mM KCl, 0.05% (v/v) Triton X-100, and 1% (v/v) DMSO. Freshly prepared hemin was then added to a final concentration of 1  $\mu\text{M}$ , and the solution was incubated for 30 minutes at room temperature. The mixture was then added to a 384-well plate, and  $\text{H}_2\text{O}_2$  (final concentration 2 mM) and ABTS (final concentration 1.5 mM) were added to initiate the reaction. The absorption intensity at  $\lambda = 418\text{ nm}$  ( $\text{ABTS}^{++}$ ) was recorded every minute using a Tecan Infinite M1000 PRO microplate reader. The concentration of  $\text{ABTS}^{++}$  was calculated based on the extinction coefficient of  $\text{ABTS}^{++}$  at  $\lambda = 418\text{ nm}$  ( $\epsilon = 36000\text{ M}^{-1}\text{cm}^{-1}$ ).<sup>1</sup> The concentration of  $\text{ABTS}^{++}$  was plotted as a function of time and the initial reaction rates ( $V_0$ ) were determined by calculating the slope of the linear portion of the plot. This parameter was used to evaluate the catalytic activity of the split duplex DNA-DNAzyme conjugates.

**Optimization of KCl and NaCl concentration.** To maximize the signal gain from our CBSAzymes, we optimized the buffer concentrations of KCl and NaCl using a two-factor, 12-level uniform design.<sup>2</sup> We tested a combination of 12 different KCl and NaCl concentrations. 5  $\mu\text{L}$  of varying concentrations of 10 $\times$  KCl and NaCl were mixed with 4  $\mu\text{L}$  of HEPES buffer (final concentration: 40 mM, pH 7.0), 13  $\mu\text{L}$  of deionized water (DI), and 2.5  $\mu\text{L}$  of each CBSAzyme fragment (final concentration of each strand: 1  $\mu\text{M}$ ). 5  $\mu\text{L}$  of cocaine or MDPV (final concentration: 250  $\mu\text{M}$ ) was then added to the mixture and the solution was incubated for 30 minutes. Afterwards, 0.5  $\mu\text{L}$  hemin (final concentration 1  $\mu\text{M}$ ) and 2.5  $\mu\text{L}$  Triton X-100 (final concentration 0.05%) were added to the mixture, and the solution was incubated for another 30 minutes. The solution was subsequently transferred into a well of a 384-well plate and then a 10  $\mu\text{L}$  of a substrate solution (final concentrations: 2 mM  $\text{H}_2\text{O}_2$ , 1.5 mM ABTS and 40 mM HEPES) was added. The absorbance at 418 nm was monitored every minute using a Tecan Infinite M1000 PRO microplate reader. The combination of salt concentrations that achieved the highest signal gain was used for subsequent experiments. The signal gain was calculated by  $A/A_0$ , where A and  $A_0$  are the absorbance values of CBSAzyme mixture with and without target, respectively.

**Determination of CBSAzyme kinetics.** The following experiments were performed at room

temperature. The Michaelis-Menten constant ( $K_M$ ) and turnover number ( $k_{cat}$ ) of the CBSAzyme were determined by varying the concentration of ABTS. Specifically, 1  $\mu$ M of each fragment was mixed with 250  $\mu$ M cocaine in 40 mM HEPES (pH 7.0) containing 0.05% Triton X-100, 1% DMSO and optimal concentrations of KCl and NaCl as determined above. This mixture was incubated for 30 minutes and then 1  $\mu$ M hemin was added. After 30 minutes of incubation, the sample was loaded into a well of a 384-well microplate and the enzymatic reaction was initiated by the addition of 2 mM  $H_2O_2$  and various concentrations of ABTS (final concentration: 0.1, 0.5, 1.0, 1.5, 2.0, 4.0, or 6.0 mM). The absorbance at 418 nm was monitored every minute using a Tecan Infinite M1000 PRO microplate reader and the corresponding absorbance values were converted to concentration using the extinction coefficient of  $ABTS^{*+}$  at  $\lambda = 418$  nm ( $\epsilon = 36000$  M<sup>-1</sup>cm<sup>-1</sup>). The concentration of  $ABTS^{*+}$  was plotted against time, and the initial reaction rates were determined by calculating the slope of the linear portion of the plot. To determine  $K_M$  and maximal velocity ( $V_{max}$ ), the initial reaction rate was plotted against the concentration of ABTS, and that plot was fitted with the Michaelis-Menten equation<sup>3</sup> using nonlinear regression.

**Characterizing binding affinity and cooperativity of MDPV-binding CBSA using a fluorescence assay.** The long fragment and fluorophore-quencher-modified short fragment of MDPV-6335 (final concentration of each: 1  $\mu$ M) was mixed with 40 mM HEPES buffer (pH 7.0) containing 7 mM KCl and 77 mM NaCl. Various concentrations of MDPV (final concentrations: 1, 3, 10, 30, 100, 300, 1000, or 3000  $\mu$ M) were added into the mixture, and the solution was incubated for 30 minutes at room temperature. The total reaction volume was 100  $\mu$ L. Each reaction was loaded into a well of a 96-well microplate and the fluorescence intensity at 668 nm was measured using a Tecan Infinite M1000 PRO microplate reader with excitation at 648 nm. The signal gain was calculated by  $(F-F_0)/F_0 \times 100\%$ , where  $F_0$  is the fluorescence of MDPV-6335 mixture without MDPV, and  $F$  is the fluorescence of MDPV-6335 mixtures with MDPV. Signal gain was plotted against the employed MDPV concentration, and the plot was fitted with the Hill equation<sup>4</sup> using Origin 2017 software to calculate the Hill coefficient ( $n_H$ ) and MDPV concentration producing half occupancy ( $K_{1/2}$ ).

**Circular dichroism characterization of CBSAzyme conformation.** Circular dichroism experiments, including sample preparation, were performed at room temperature. For cocaine, 1  $\mu$ M of each CBSAzyme fragment was incubated with or without 250  $\mu$ M cocaine in 40 mM HEPES buffer (pH 7.0) containing 1% DMSO, and optimal KCl and NaCl concentrations (listed under respective circular dichroism figures in ESI) for 30 minutes. Hemin (final concentration 1  $\mu$ M) or DMSO (for control experiments, final concentration 1% (v/v) for control experiments) was added, and the solution was incubated for another 30 minutes. The samples (300  $\mu$ L) were transferred into a 1 cm quartz cuvette (Hellma Analytics) to perform circular dichroism measurements using a Jasco J-815 circular dichroism spectropolarimeter with scan range: 235 to 300 nm, scanning speed: 50 nm/min, sensitivity: 100 mdeg, response time: 1 s, bandwidth: 1 nm, total scans: 6. For MDPV, hemin (final concentration 1  $\mu$ M) or DMSO (for control experiments, final concentration 1% (v/v)) was added to 1  $\mu$ M of each MDPV-CBSAzyme fragment with or without 200  $\mu$ M MDPV in 40 mM HEPES buffer (pH 7.0) containing 1% DMSO, 7 mM KCl, and 77 mM NaCl. The mixture was incubated overnight at room temperature. The circular dichroism spectra were recorded with scan range: 220 to 300 nm, scanning speed: 50 nm/min, sensitivity: 5 mdeg, response time: 8 s, bandwidth: 1 nm, total scans: 6. For data analysis, all circular dichroism spectra were averaged and then corrected by subtracting the circular dichroism spectra of the reaction buffer with or without drug.

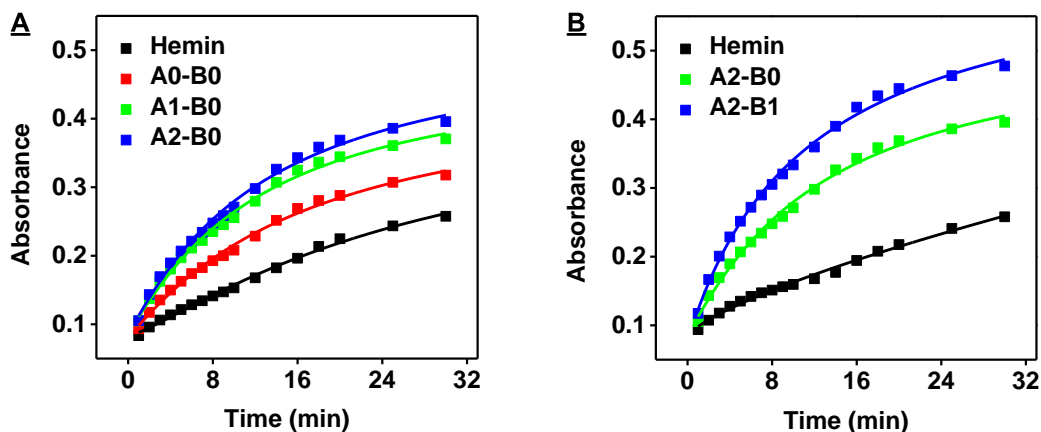


**Figure S1.** Optimization of the catalytic activity of duplex DNA-split DNAzyme conjugates. Time-course measurement of absorbance at 418 nm using split DNAzymes with (A) strand B0 and different variants of strand A and (B) strand A2 and different variants of strand B. Hemin alone was used as a control.

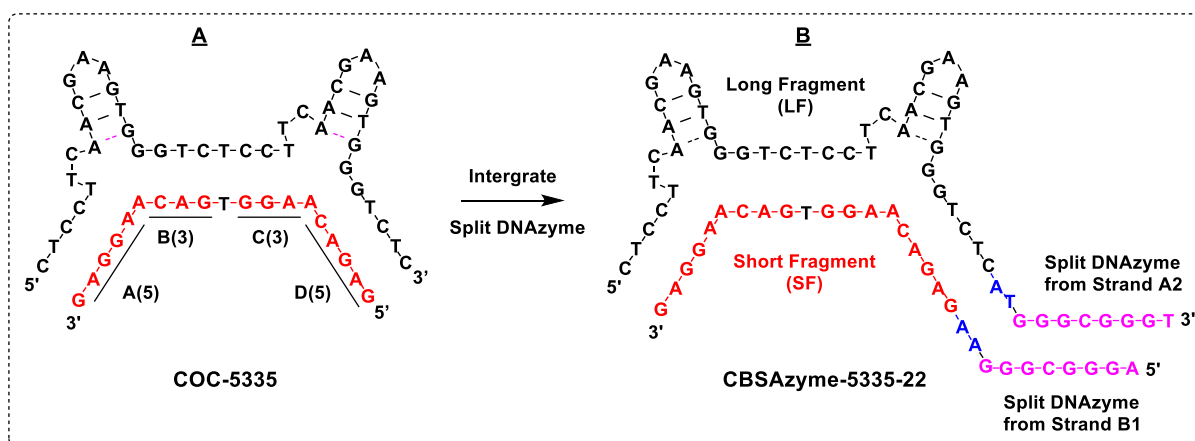


**Figure S2.** Strategy for engineering the cocaine-binding CBSAzyme from a cocaine-binding CBSA. The split DNAzyme segments from strands A2 and B1 are conjugated to the ends of (A) COC-5335 to generate (B) CBSAzyme-5335-22.

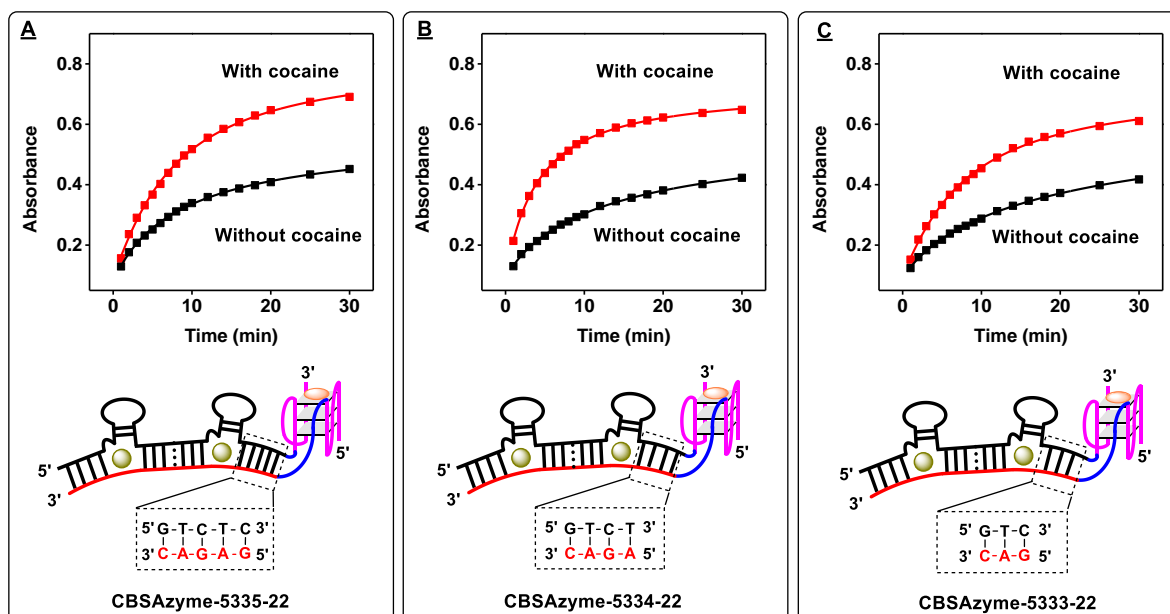


**Figure S3.** Effect of CBSA stem-length on the performance of the cocaine-detecting CBSAzyme. Time-course of absorbance measurements for (A) CBSAzyme-5335, (B) CBSAzyme-5334, (C) CBSAzyme-5333 in the presence and absence of 250  $\mu\text{M}$  cocaine. [Each fragment] = 0.25  $\mu\text{M}$ .

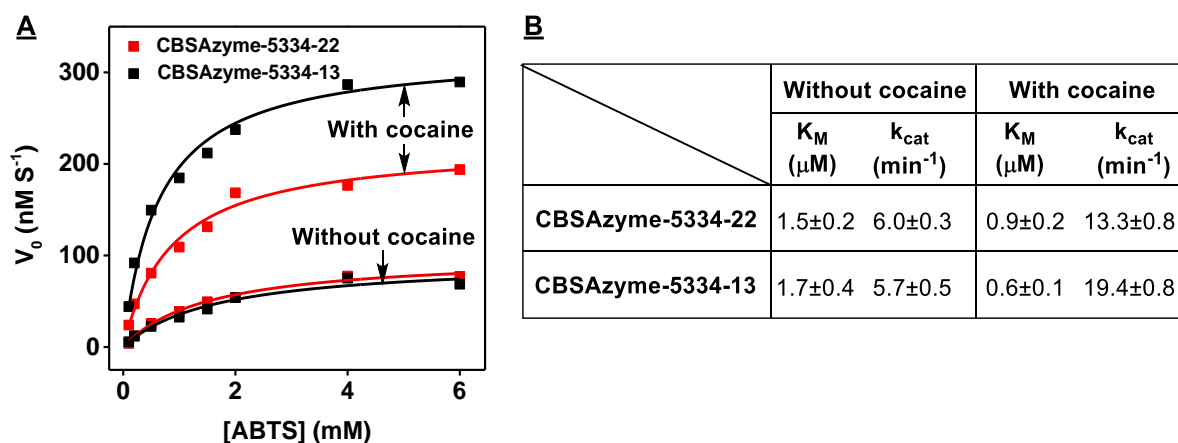


**Figure S4.** Determination of the enzyme kinetics of CBSAzyme-5334-22 and CBSAzyme-5334-13. (A) The initial reaction rate of the CBSAzymes was plotted against the concentration of ABTS. (B) The Michaelis-Menten constant ( $K_m$ ) and turnover number ( $k_{\text{cat}}$ ) in the presence and absence of cocaine were obtained from the plotted curve.

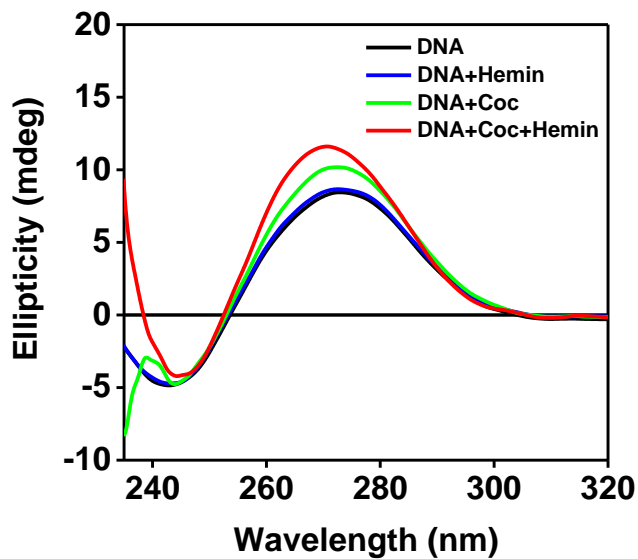


**Figure S5.** Circular dichroism spectra of 1  $\mu\text{M}$  CBSAzyme-5334-13 alone (black) or with 250  $\mu\text{M}$  cocaine (green), 1  $\mu\text{M}$  hemin (blue), or both (red). Circular dichroism contributions from cocaine and hemin were subtracted. Buffer conditions: 40 mM HEPES (pH 7.0), 2 mM KCl, 28 mM NaCl, 1% (v/v) DMSO.

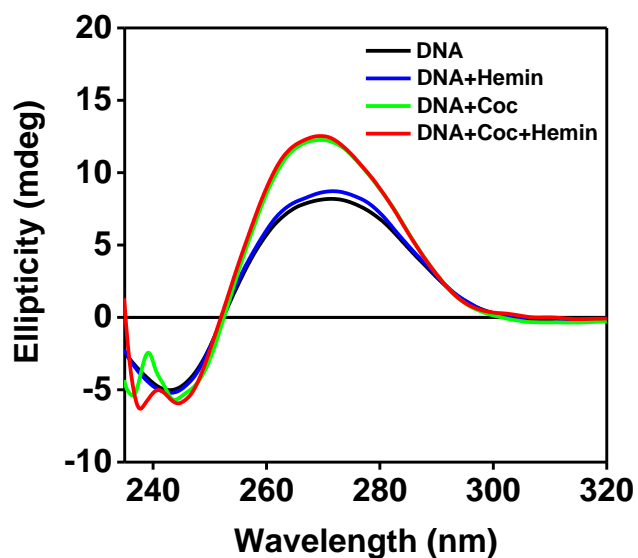


**Figure S6.** Circular dichroism spectra of 1  $\mu\text{M}$  CBSAzyme-5334-22 alone (black) as well as with 250  $\mu\text{M}$  cocaine (green), 1  $\mu\text{M}$  hemin (blue), or both (red). Circular dichroism contributions from cocaine and hemin were subtracted. Buffer conditions: 40 mM HEPES (pH 7.0), 7 mM KCl, 7 mM NaCl, 1% DMSO.

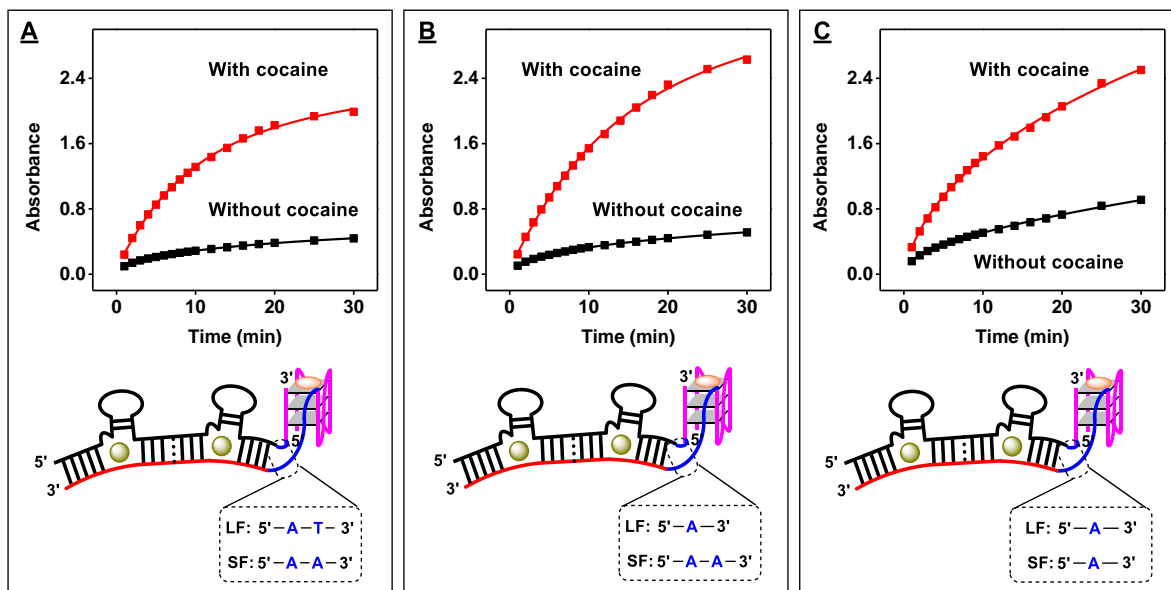


**Figure S7.** Optimization of the linker of CBSAzyme-5334-13. Structure and time-course of CBSAzyme-5334-13 with linkers comprising (A) AT/AA, (B) A/AA, and (C) A/A in the absence and presence of 250  $\mu\text{M}$  cocaine. The absorbance at 418 nm was recorded over 30 minutes. [Each fragment] = 1  $\mu\text{M}$ .

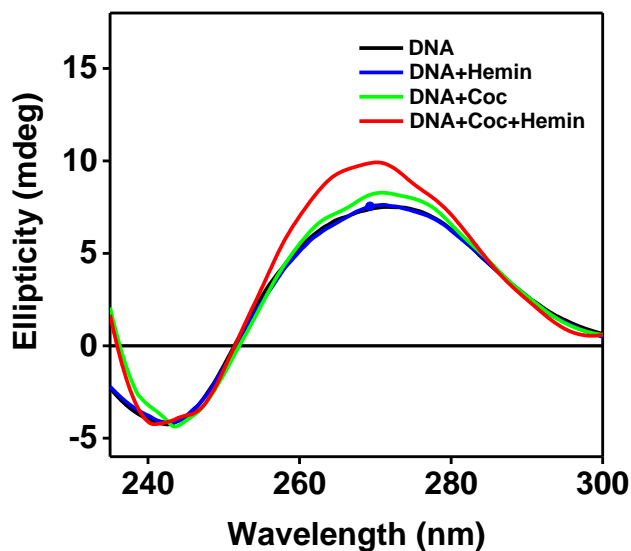


**Figure S8.** Circular dichroism spectra of 1  $\mu\text{M}$  COC-CBSAzyme alone (black) as well as with 250  $\mu\text{M}$  cocaine (green), 1  $\mu\text{M}$  hemin (blue), or both (red). Circular dichroism contributions from cocaine and hemin were subtracted. Buffer conditions: 40 mM HEPES (pH 7.0), 1 mM KCl, 30 mM NaCl, 1% DMSO.



### Experimental Setup

Components	Sample Number					
	1	2	3	4	5	6
HEPES buffer	+	+	+	+	+	+
H <sub>2</sub> O <sub>2</sub> and ABTS	+	+	+	+	+	+
Hemin		+	+	+	+	+
COC-CBSAzyme-SF			+		+	+
COC-CBSAzyme-LF				+	+	+
Cocaine						+



**Figure S9.** Utilizing COC-CBSAzyme for the naked-eye detection of cocaine. Experimental setup shows sample contents and photographs depict the color of the samples containing (1) reaction buffer alone, (2) 1  $\mu\text{M}$  hemin alone, (3) 1  $\mu\text{M}$  short fragment with hemin, (4) 1  $\mu\text{M}$  long fragment with hemin, and both fragments in the (5) absence and (6) presence of 250  $\mu\text{M}$  cocaine after 15 minutes of reaction.

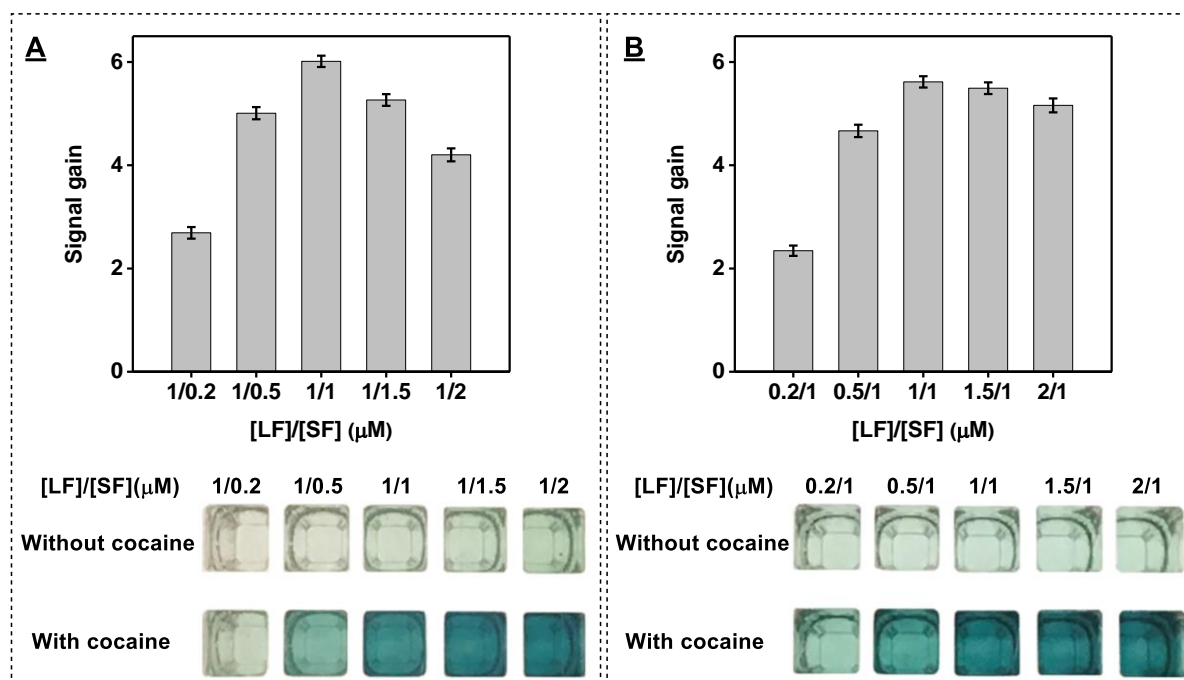


**Figure S10.** Optimization of the concentrations of the long and short fragments of COC-CBSAzyme in the CBSAzyme-based colorimetric assay. The assay was performed in the presence and absence of 250  $\mu\text{M}$  cocaine with (A) 1  $\mu\text{M}$  long fragment and 0.2, 0.5, 1, 1.5 or 2  $\mu\text{M}$  of short fragment, or (B) 0.2, 0.5, 1, 1.5 or 2  $\mu\text{M}$  long fragment and 1  $\mu\text{M}$  of short fragment. Top panels show the signal gain obtained with various ratios of long and short fragment after 15 minutes of reaction. Bottom panels are photographs depicting the color of the samples.

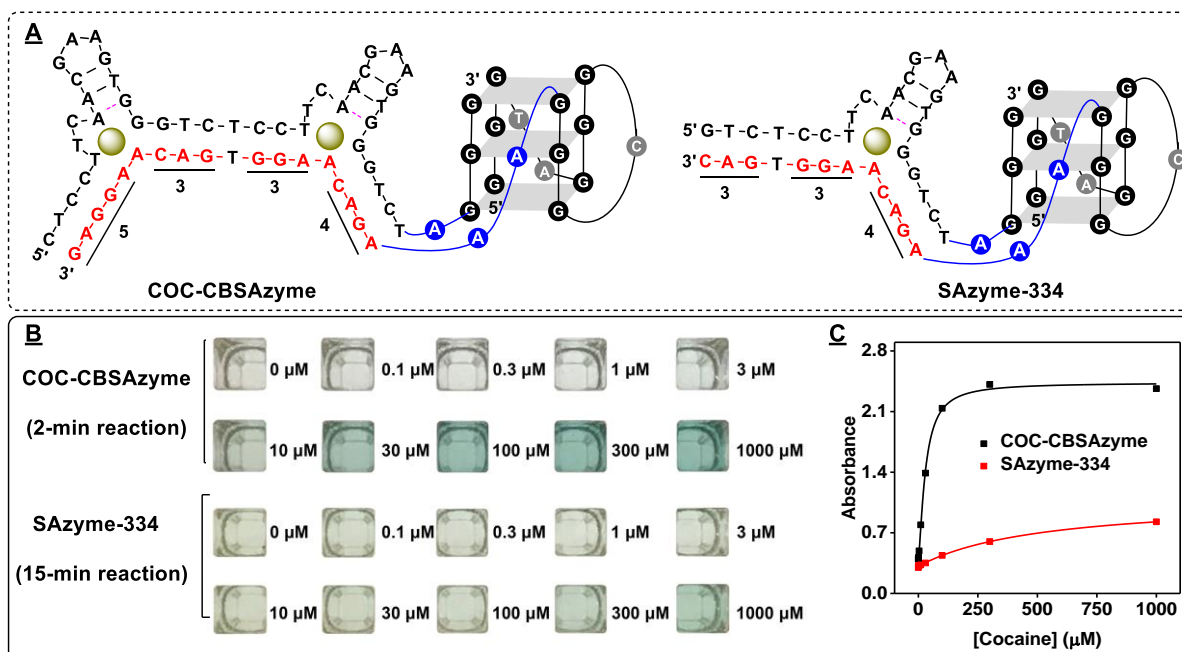


**Figure S11.** Comparison of the target-responsiveness of COC-CBSAzyme and SAzyme-334. (A) Structures of COC-CBSAzyme and SAzyme-334. (B) Photographs and (C) calibration curves of samples containing COC-CBSAzyme and SAzyme-334 in the presence of various concentrations of cocaine (0 – 1000  $\mu\text{M}$ ) after 2 minutes and 15 minutes of reaction, respectively.

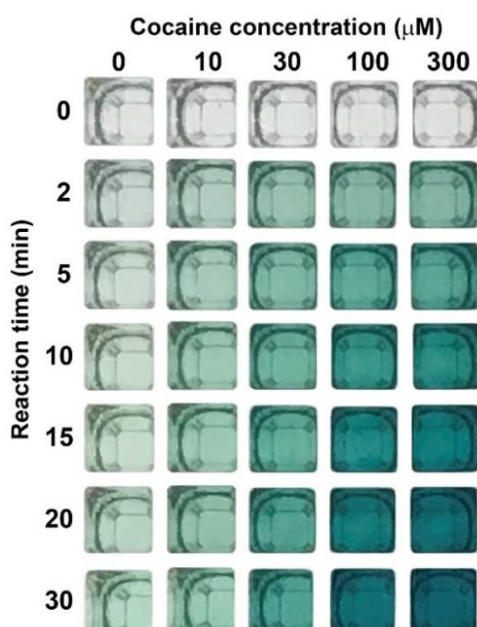


**Figure S12.** Visual detection of cocaine using COC-CBSAzyme. Photographs of the samples containing different concentrations of cocaine (0 – 300  $\mu\text{M}$ ) at different time points (0 – 30 min). The color of the cocaine-containing samples progressively changes over time.

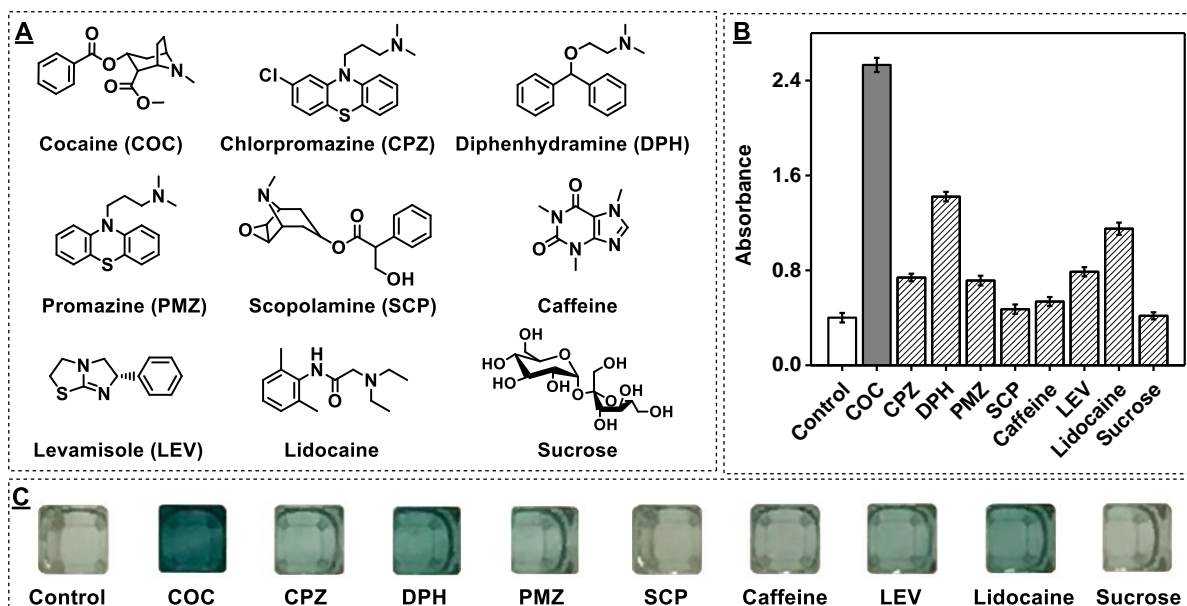


**Figure S13.** Specificity of the CBSAzyme-based assay for cocaine detection. (A) Chemical structures of interferents tested in the assay. (B) Absorbance of samples at 418 nm after 15 minutes of reaction containing various interferents (250  $\mu$ M). (C) Photographs of samples containing various interferents (250  $\mu$ M) after 15 minutes of reaction.

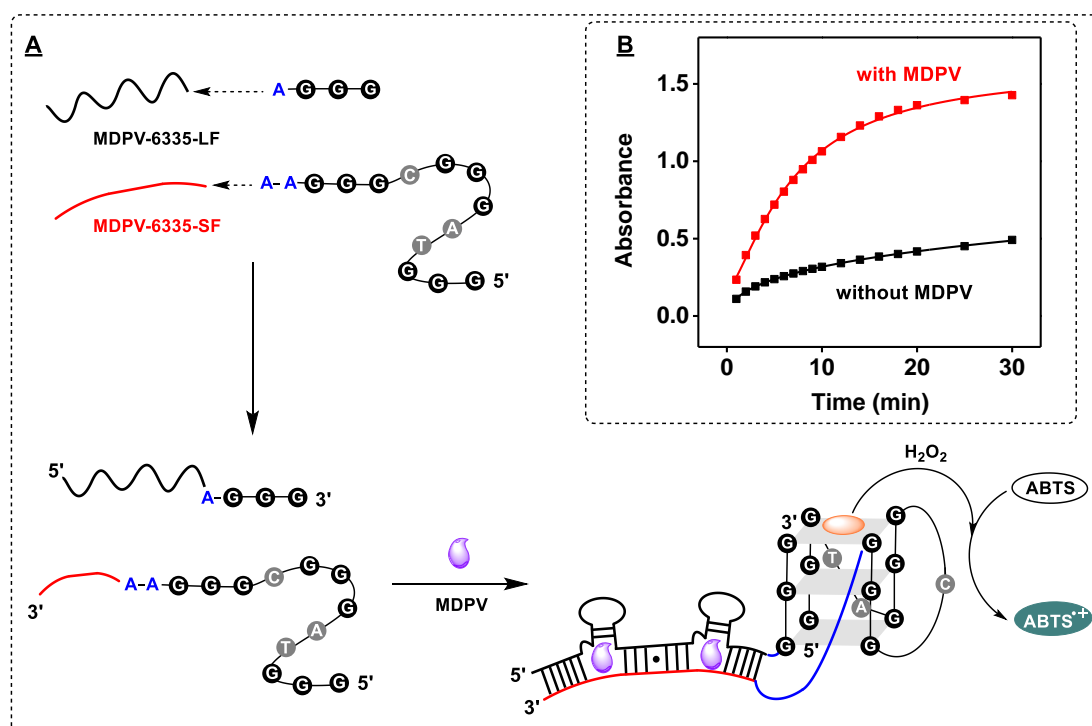


**Figure S14.** Design and performance of an MDPV-binding CBSAzyme. (A) Engineering of MDPV-CBSAzyme using MDPV-6335 and the optimized split DNAzyme fragments. In the presence of MDPV, the two CBSAzyme fragments assemble, such that the DNAzyme can catalyze the oxidation of ABTS to generate the green-colored ABTS radical. (B) Time-course absorbance measurement at 418 nm with reaction buffer containing 1  $\mu$ M MDPV-CBSAzyme in the presence and absence of 250  $\mu$ M MDPV.

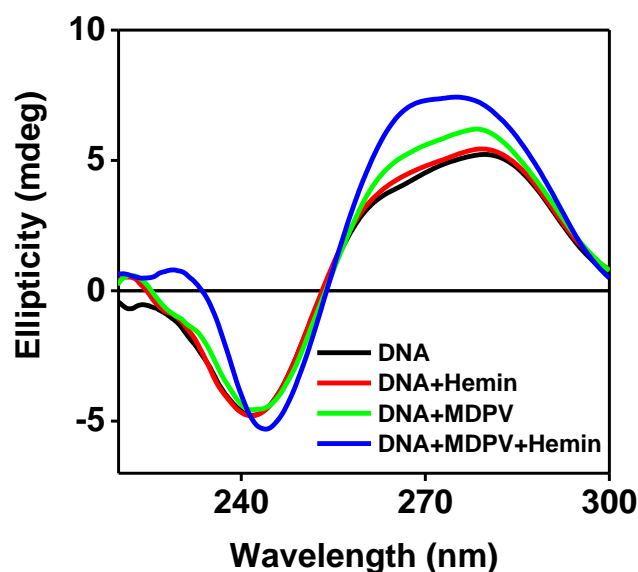


**Figure S15.** Circular dichroism spectra of 1  $\mu\text{M}$  MDPV-CBSAzyme alone (black) and with 200  $\mu\text{M}$  MDPV (green), 1  $\mu\text{M}$  hemin (red), or both (blue). Circular dichroism contributions from MDPV and hemin were subtracted. Buffer conditions: 40 mM HEPES pH 7, 7 mM KCl, 77 mM NaCl, 1% DMSO.

### Experimental Setup

Components	Sample Number					
	1	2	3	4	5	6
HEPES buffer	+	+	+	+	+	+
H <sub>2</sub> O <sub>2</sub> and ABTS	+	+	+	+	+	+
Hemin			+	+	+	+
MDPV-CBSAzyme-SF				+	+	+
MDPV-CBSAzyme-LF					+	+
MDPV						+



**Figure S16.** Utilizing MDPV-CBSAzyme for the naked-eye detection of MDPV. Experimental setup shows sample contents and photographs depict the color of the samples containing (1) reaction buffer alone, (2) 1  $\mu\text{M}$  hemin alone, (3) 1  $\mu\text{M}$  short fragment with hemin, (4) 1  $\mu\text{M}$  long fragment with hemin, and both fragments in the (5) absence and (6) presence of 250  $\mu\text{M}$  MDPV after 15 minutes of reaction.

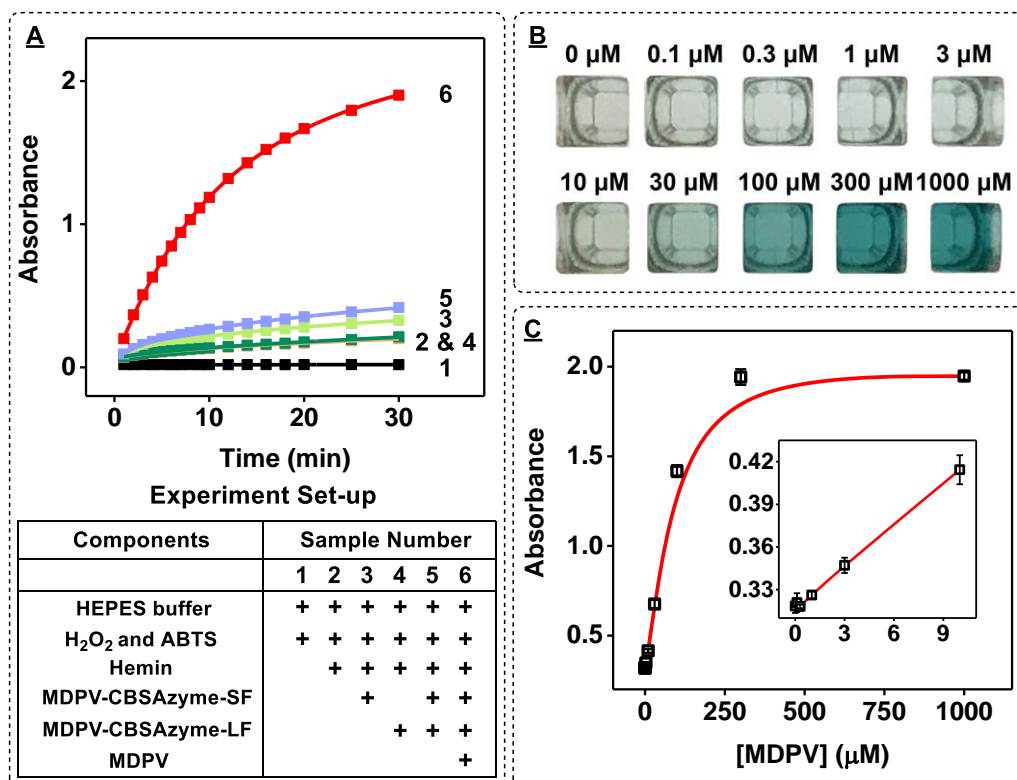


**Figure S17.** Visual detection of MDPV based on MDPV-CBSAzyme. (A) Time-dependent absorbance change at 418 nm with (1) reaction buffer alone, (2) hemin alone, (3) the short fragment plus hemin, (4) the long fragment with hemin, and both fragments in the (5) absence or (6) presence of 250  $\mu\text{M}$  MDPV. (B) Photographs of samples containing different concentrations of MDPV after 15 minutes of reaction. (C) Assay calibration curve with MDPV concentrations (0 to 1,000  $\mu\text{M}$ ). Inset represents linear range from 0 to 10  $\mu\text{M}$ . [Each fragment] = 1  $\mu\text{M}$ .

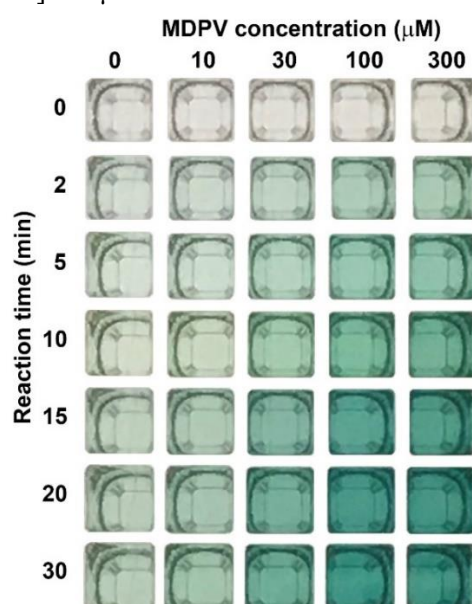


**Figure S18.** The time course visual detection of MDPV using MDPV-CBSAzyme. Photographs of the samples containing different concentrations of MDPV (0 – 300  $\mu\text{M}$ ) at different time points (0 – 30 min). The color of the MDPV-containing samples progressively changes over time.

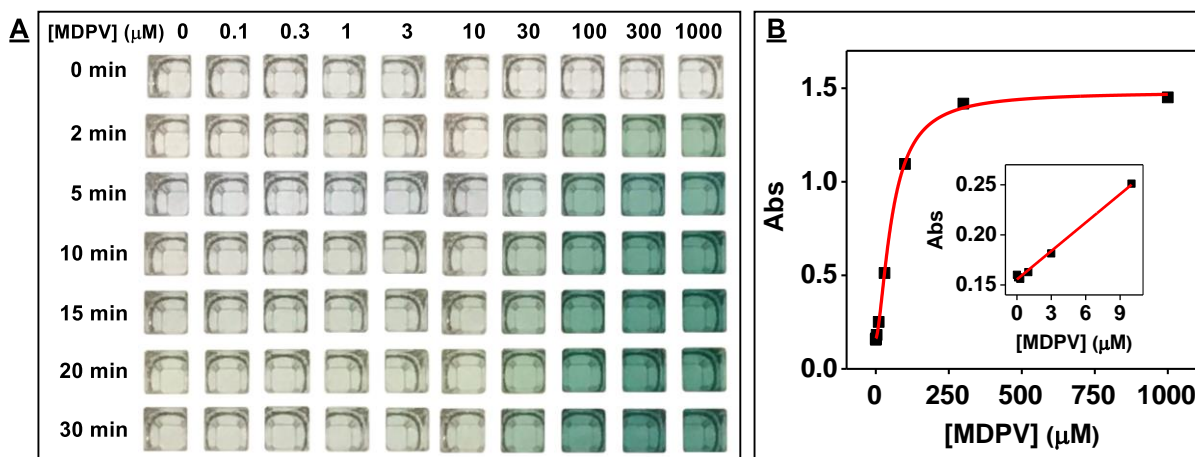


**Figure S19.** The time-course visual detection of MDPV in 50% saliva using MDPV-CBSAzyme. (A) Photographs of the samples containing different concentrations of MDPV (0 – 1000  $\mu\text{M}$ ) at different time points (0 – 30 min) are shown. The color of the MDPV-containing samples progressively changes over time, while the color of the MDPV-free sample only changed slightly. (B) Calibration curve generated using 0–1000  $\mu\text{M}$  MDPV after 15 minutes of reaction.

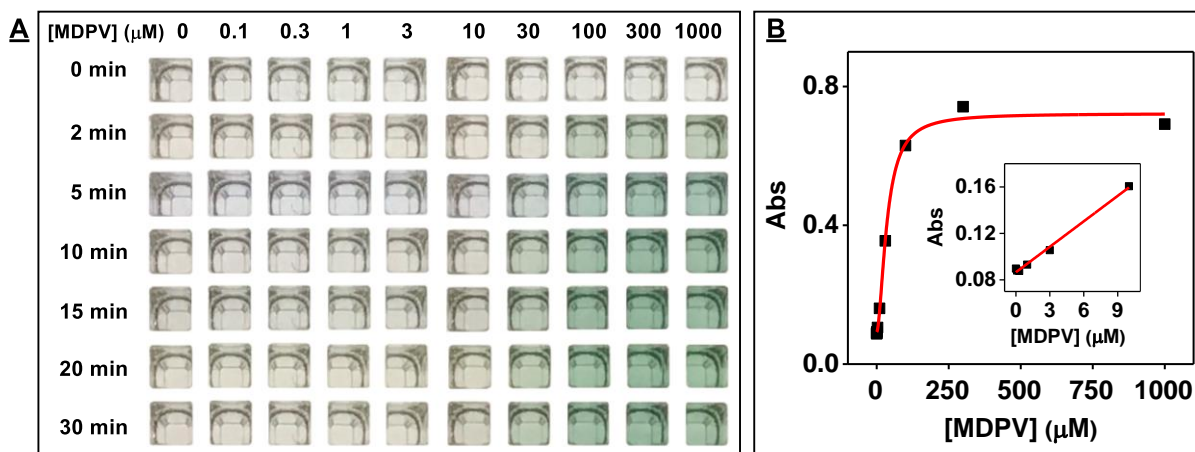


**Figure S20.** The time-course visual detection of MDPV in 50% urine using MDPV-CBSAzyme. (A) Photographs of the samples containing different concentrations of MDPV (0 – 1000  $\mu\text{M}$ ) at different time points (0 – 30 min) are shown. The color of the MDPV-containing samples progressively changes over time, while the color of the MDPV-free sample only changed slightly. (B) Calibration curve generated using 0–1000  $\mu\text{M}$  MDPV after 15 minutes of reaction.

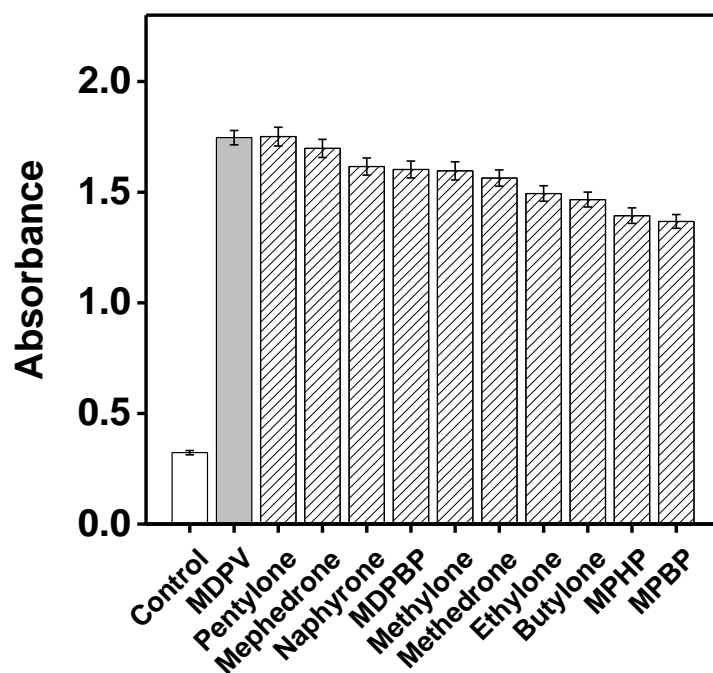


**Figure S21.** Target-cross-reactivity of the MDPV-CBSAzyme-based assay. Absorbance of samples at 418 nm after 15 minutes for samples containing 11 different synthetic cathinones at a concentration of 250  $\mu$ M.

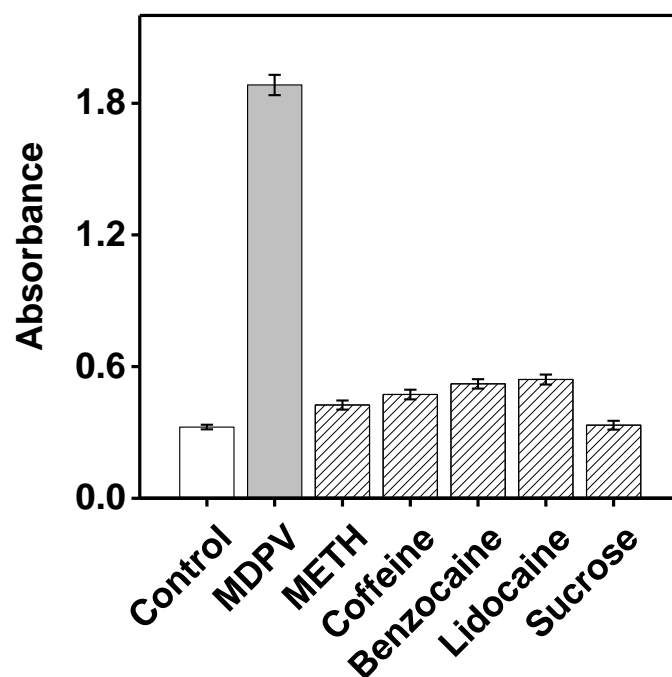


**Figure S22.** Specificity of the MDPV-CBSAzyme-based assay. Absorbance of samples at 418 nm after 15 minutes for samples containing various interferents (250  $\mu$ M). MDPV is shown as a positive control.

**Table S1.** Oligonucleotide sequences used in this work.

Sequence ID	Sequence (5'-3')
Strand A0	AGT AAC AAC AAT CAA AAT ATG TGG AGG GT
Strand A1	AGT AAC AAC AAT CAA AAT ATG GGA GGG T
Strand A2	AGT AAC AAC AAT CAA AAT ATG GGC GGG T
Strand B0	AGG GAC GGG AAA TTT TGA TTG TTG TTA CT
Strand B1	AGG GCG GGA AAT TTT GAT TGT TGT TAC T
COC-5335 Long Fragment	CTC CTT CAA CGA AGT GGG TCT CCT TCA ACG AAG TGG GTC TC
COC-5335 Short Fragment	GA GAC AAG GTG ACA AGG AG
COC-CBSAzyme-5335-22-LF	CTC CTT CAA CGA AGT GGG TCT CCT TCA ACG AAG TGG GTC TCA TGG GCG GGT
COC-CBSAzyme-5335-22-SF	AGG GCG GGA AGA GAC AAG GTG ACA AGG AG
COC-CBSAzyme-5334-22-LF	CTC CTT CAA CGA AGT GGG TCT CCT TCA ACG AAG TGG GTC TAT GGG CGG GT
COC-CBSAzyme-5334-22-SF	AGG GCG GGA AAG ACA AGG TGA CAA GGA G
COC-CBSAzyme-5333-22-LF	CTC CTT CAA CGA AGT GGG TCT CCT TCA ACG AAG TGG GTC ATG GGC GGG T
COC-CBSAzyme-5333-22-SF	AGG GCG GGA AGA CAA GGT GAC AAG GAG
COC-5334-SF	AG ACA AGG TGA CAA GGA G
COC-5334-LF	CTC CTT CAA CGA AGT GGG TCT CCT TCA ACG AAG TGG GTC T
COC-CBSAzyme-5334-13-LF (AT linker)	CTC CTT CAA CGA AGT GGG TCT CCT TCA ACG AAG TGG GTC TAT GGG
COC-CBSAzyme-5334-13-SF (AA linker)	GGG TAG GGC GGG AAA GAC AAG GTG ACA AGG AG
COC-CBSAzyme-5334-13-LF (A linker)	CTC CTT CAA CGA AGT GGG TCT CCT TCA ACG AAG TGG GTC TAG GG
COC-CBSAzyme-5334-13-SF (A linker)	GGG TAG GGC GGG AAG ACA AGG TGA CAA GGA G
SAzyme-334-LF	GTC TCC TTC AAC GAA GTG GGT CTA GGG
SAzyme-334-SF	GGG TAG GGC GGG AAA GAC AAG GTG AC
MDPV-Binding Aptamer	CTT ACG ACT CAG GCA TTT TGC CGG GTA ACG AAG TTA CTG TCG TAA G
MDPV-6335-LF	TAC GAC TCA GGC TTT GCC GGG TAT GAC TCA GGC TTT GCC GGG TAA C
MDPV-6335-SF	G TTA CTG TCT TAC TGT CGT A
MDPV-6335-SF-FQ	/5IAbRQ/ G TTA CTG TCT TAC TGT CGT A /3Cy5Sp/
MDPV-CBSAzyme-LF	TAC GAC TCA GGC TTT GCC GGG TAT GAC TCA GGC TTT GCC GGG TAA CAG GG
MDPV-CBSAzyme-SF	GGG TAG GGC GGG AAG TTA CTG TCT TAC TGT CGT A

/5IAbRQ/ represents IowaBlack RQ quencher

/3Cy5Sp/ represents Cy5 fluorophore



**Table S2.** Comparison of the CBSAzyme-based assay to other aptamer-based assays for colorimetric cocaine detection.

Sensing element	Label free	Enzyme free	LOD ( $\mu\text{M}$ )	Visual LOD ( $\mu\text{M}$ )	Turnaround time	On-site Usability	Ref
CBSAzymes	Yes	Yes	1	10	5 min	Yes	This work
Split-aptamer-DNAzyme conjugates	No	Yes	0.05	0.1	2 hrs	No	1
Split-aptamer DNAzyme conjugates	Yes	Yes	1	N/A	15 min	No	2
Aptamer-DNAzyme conjugates	Yes	Yes	5	1000	1 h	No	3
Enzyme-linked split aptamer	No	No	0.1	NA	2 hrs	No	4
Aptamer crosslinked AuNPs	No	No	2	10	30 min	No	5
Aptamer-modified AuNPs	No	Yes	50	1000	1 min	No	6
Aptamer-dye complex	Yes	Yes	2	500	12 hrs	No	7
Aptamer-crosslinked hydrogel	No	No	2	2	10 min	No	8

#### References:

- (1) Du, Y.; Li, B.; Guo, S.; Zhou, Z.; Zhou, M.; Wang, E.; Dong, S. G-Quadruplex-Based DNAzyme for Colorimetric Detection of Cocaine: Using Magnetic Nanoparticles as the Separation and Amplification Element. *Analyst* **2011**, *136*, 493–497.
- (2) Elbaz, J.; Moshe, M.; Shlyahovsky, B.; Willner, I. Cooperative Multicomponent Self-Assembly of Nucleic Acid Structures for the Activation of DNAzyme Cascades: A Paradigm for DNA Sensors and Aptasensors. *Chem. - Eur. J.* **2009**, *15*, 3411–3418.
- (3) Nie, J.; Zhang, D. W.; Tie, C.; Zhou, Y. L.; Zhang, X. X. A Label-Free DNA Hairpin Biosensor for Colorimetric Detection of Target with Suitable Functional DNA Partners. *Biosens. Bioelectron.* **2013**, *49*, 236–242.
- (4) Sharma, A. K.; Kent, A. D.; Heemstra, J. M. Enzyme-Linked Small-Molecule Detection Using Split Aptamer Ligation. *Anal. Chem.* **2012**, *84*, 6104–6109.
- (5) Yu, H.; Canoura, J.; Guntupalli, B.; Alkhamis, O.; Xiao, Y. Sensitive Detection of Small-Molecule Targets Using Cooperative Binding Split Aptamers and Enzyme-Assisted Target Recycling. *Anal. Chem.* **2018**, *90*, 1748–1758.
- (6) Liu, J.; Lu, Y. Fast Colorimetric Sensing of Adenosine and Cocaine Based on a General Sensor Design Involving Aptamers and Nanoparticles. *Angew. Chem., Int. Ed.* **2006**, *45*, 90–94.
- (7) Stojanovic, M. N.; Landry, D. W. Aptamer-Based Colorimetric Probe for Cocaine. *J. Am. Chem. Soc.* **2002**, *124*, 9678–9679.
- (8) Zhu, Z.; Wu, C.; Liu, H.; Zou, Y.; Zhang, X.; Kang, H.; Yang, C. J.; Tan, W. An Aptamer Cross-Linked Hydrogel as a Colorimetric Platform for Visual Detection. *Angew. Chem., Int. Ed.* **2010**, *49*, 1052–1056.